

Synthesis, Structure, and DFT Calculation of (Phosphino-*o*-carboranyl)silyl Group 10 Metal Complexes: Formation of Stable *trans*-Bis(*P,Si*-chelate)metal Complexes

Young-Joo Lee,[†] Jong-Dae Lee,[†] Sung-Joon Kim,[†] Samrok Keum,[†] Jaejung Ko,^{*,†} Il-Hwan Suh,[†] Minserk Cheong,[‡] and Sang Ook Kang^{*,†,§}

Department of Chemistry, Korea University, 208 Seochang, Chochiwon, Chung-nam 339-700, Korea, and Department of Chemistry and Research Institute for Basic Sciences, Kyung Hee University, Seoul 130-701, Korea

Received August 14, 2003

Addition of the silane (HSiMe₂)C₂B₁₀H₁₀(PR₂) (R = Me (**2a**), OEt (**2b**)) to (PPh₃)₂Pt(CH₂-CH₂) (**3**) affords the *trans*-bis(chelates) Pt(Cab^{*P,Si*})₂ (**4a,b**; Cab^{*P,Si*} = η²-[(SiMe₂)(PR₂)C₂B₁₀H₁₀-*P,Si*]) in high yield; the same product was also formed from Pt(cod)₂ (**9**), as confirmed by NMR spectroscopy (¹H, ³¹P). Using Pd₂(dba)₃ (**6**), the analogue *trans*-bis(chelate) Pd(Cab^{*P,Si*})₂ (**7a**) was obtained as a mixture of *trans* and *cis* isomers in which the former predominates, as established by NMR spectroscopy (¹H, ³¹P). Thus, a series of kinetically stabilized *trans*-bis(chelate) metal complexes, *trans*-(Cab^{*P,Si*})₂M (M = Pt (**4a,b**), Pd (**7a**)), bearing bulky *o*-carboranylphosphine tethers, were synthesized from the reaction of phosphinosilanes (**2**) with d¹⁰ metal complexes. In the presence of dimethyl acetylenedicarboxylate (DMAD), the *trans* isomer **4a,b** thermally rearranges to the thermodynamically favored *cis* isomer *cis*-(Cab^{*P,Si*})₂Pt (**5a,b**). In addition, the oxidative addition of the Si–H bond to the sterically bulky diphenylphosphino silane (HSiMe₂)C₂B₁₀H₁₀(PPh₂) (**2c**) by **3** can be controlled to produce the mono(chelate) species (Cab^{*P,Si*})Pt(H)(PPh₃) (**10a**). The related mono(chelate) product (Cab^{*P,Si*})Pt(H)(Cab^{*P*}) (**10b**; Cab^{*P*} = (PPh₂)C₂B₁₀H₁₁) results from the oxidative addition of **2c** by **3**, in which one PPh₃ ligand is displaced by Cab^{*P*}. The structures of compounds **4a**, **5a,c**, **8c**, and **10a,b** were determined using single-crystal X-ray crystallography.

Introduction

(Phosphinoalkyl)silanes are used as chelate ligands in a wide range of oxidative addition reaction processes with transition metals¹ and have been studied in considerable detail, principally to obtain a better understanding of industrially important metal-catalyzed reactions such as hydrosilylation.² Such molecules undergo oxidative addition at low-valent transition-metal centers in which Si–M bond formation is accompanied by chelation with phosphine donors, affording ((phosphinoalkyl)silyl)metal complexes. Although many examples of bis(chelate) metal complexes with a *cis* arrangement of the (phosphinoalkyl)silyl ligands in a typical square-planar M(II) (M = Pd, Pt) environment have been synthesized³ and evaluated in the aforemen-

tioned context, comparatively few *trans*-bis(chelates)^{3c} have received scrutiny, principally because of their inaccessibility. Recent reports of unusually stable cyclic bis(*o*-carboranylsilyl)metal complexes⁴ appear to imply that the properties of these complexes, such as their chelation, rigid conformation, and *o*-carboranyl ligand backbones might be ideal for the kinetic stabilization of metal silyl intermediates in the double-silylation process.⁵ Therefore, to increase the kinetic stability of this type of ligand framework, we have synthesized (phosphinoalkyl)silane precursors with a two-carbon skeleton connecting the silicon and phosphorus atoms that is part of a bulky *o*-carboranyl unit. These new (phosphino-*o*-carboranyl)silanes were used in this study to isolate a series of *trans*-bis(chelate)metal complexes, which are formed by “chelate-assisted” oxidative addi-

[†] Korea University.

[‡] Kyung Hee University.

[§] Tel: +82-41-860-1334. Fax: +82-41-867-5396. E-mail: sangok@korea.ac.kr.

(1) (a) Okazaki, M.; Ohshitanai, S.; Iwata, M.; Tobita, H.; Ogino, H. *Coord. Chem. Rev.* **2002**, *226*, 167. (b) Brost, R. D.; Bruce, G. C.; Joslin, F. L.; Stobart, S. R. *Organometallics* **1997**, *16*, 5669. (c) Joslin, F. L.; Stobart, S. R. *Inorg. Chem.* **1993**, *32*, 2221. (d) Ang, H. G.; Chang, B.; Kwik, W. L. *J. Chem. Soc., Dalton Trans.* **1992**, 2161. (e) Joslin, F. L.; Stobart, S. R. *J. Chem. Soc., Chem. Commun.* **1989**, 504. (f) Holmes-Smith, R. D.; Stobart, S. R.; Vefghi, R.; Zaworotko, M. J.; Jochem, K.; Cameron, T. S. *J. Chem. Soc., Dalton Trans.* **1987**, 969. (g) Auburn, M. J.; Stobart, S. R. *Inorg. Chem.* **1985**, *24*, 318. (h) Auburn, M. J.; Holmes-Smith, R. D.; Stobart, S. R. *J. Am. Chem. Soc.* **1984**, *106*, 1314.

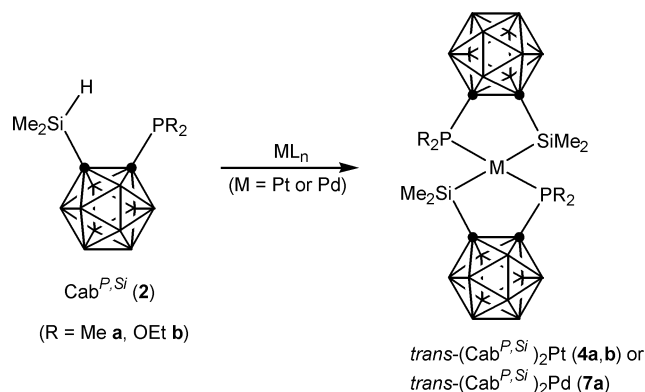
(2) (a) Speier, J. L. *Adv. Organomet. Chem.* **1979**, *407*. (b) Chalk, A. J.; Harrod, J. F. *J. Am. Chem. Soc.* **1965**, *87*, 16.

(3) (a) Gossage, R. A.; McLennan, G. D.; Stobart, S. R. *Inorg. Chem.* **1996**, *35*, 1729. (b) Grundy, S. L.; Holmes-Smith, R. D.; Stobart, S. R.; Williams, M. A. *Inorg. Chem.* **1991**, *30*, 3333. (c) Schubert, U.; Muller, C. J. *Organomet. Chem.* **1989**, *373*, 165. (d) Holmes-Smith, R. D.; Stobart, S. R.; Cameron, T. S.; Jochem, K. *J. Chem. Soc., Chem. Commun.* **1981**, 937.

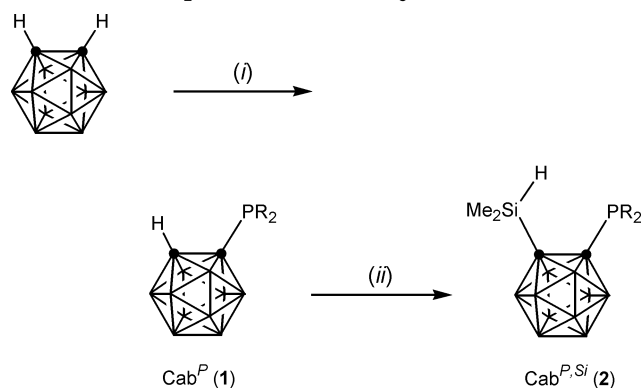
(4) (a) Kang, Y.; Ko, J.; Kang, S. O. *Organometallics* **2000**, *19*, 1216. (b) Kang, Y.; Ko, J.; Kang, S. O. *Organometallics* **1999**, *18*, 1818. (c) Kang, Y.; Lee, J.; Kong, Y. K.; Ko, J.; Kang, S. O. *Chem. Commun.* **1998**, 2343.

(5) (a) Uchimarui, Y.; Lautenschlager, H. J.; Wynd, A. J.; Tanaka, M.; Goto, M. *Organometallics* **1992**, *11*, 2639. (b) Tanaka, M.; Uchimarui, Y.; Lautenschlager, H. J. *Organometallics* **1991**, *10*, 16. (c) Eaborn, C.; Metham, T. N.; Pidcock, A. *J. Organomet. Chem.* **1973**, *63*, 107.

Scheme 1. Selective Formation of *trans*-Bis(*P,Si*-chelate)metal Complexes **4a,b and **7a****



Scheme 2. Synthesis of (Phosphino-*o*-carboranyl)silane **2^a**



^a Conditions: (i) (a) Bu^tLi , THF, -78 °C; (b) R_2PCL (R = Me **(a)**, OEt **(b)**, Ph **(c)**), THF, -78 °C; (ii) (a) Bu^tLi , THF, -78 °C; (b) Me_2SiHCl , THF, -78 °C.

tion at palladium or platinum, as shown in Scheme 1. The early results of this study have previously been communicated.⁶

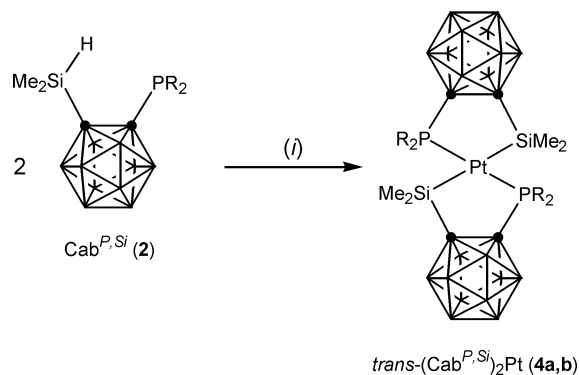
Results and Discussions

Preparation of (Phosphino-*o*-carboranyl)silanes (2**).** The (phosphino-*o*-carboranyl)silanes (**2**) were synthesized according to Scheme 2. A synthetic route to **2** is provided by the action of 1-lithio-*o*-carborane on chlorodialkylphosphine. This route affords 1-(dialkylphosphino)-*o*-carborane (**1**) in good yield as a colorless solid; then lithiation of **1** at low temperature followed by reaction with dimethylchlorosilane produces **2** (Scheme 2). A wide variety of (phosphino-*o*-carboranyl)silanes (**2**) with a Si-H bond were synthesized in this way as ligand precursors.

Each product (**2a-c**) was recovered as a colorless, rather waxy solid in ca. 82–92% yield; survival of the silyl (i.e. Si-H) functionality was obvious from the strong IR absorptions of these products near 2162–2170 cm^{-1} and from the observation of 1H NMR signals at δ 4.32 (**2a**), 4.31 (**2b**), and 4.50 (**2c**) ($\delta(Si-H)$) as multiplets that were integrated correctly vs alkyl or aryl protons. Further characterization was provided by the ^{13}C NMR (alkyl or aryl carbons) and ^{31}P NMR chemical shifts (Table 1).

(6) Lee, Y.-J.; Bae, J.-Y.; Kim, S.-J.; Ko, J.; Choi, M.-G.; Kang, S. O. *Organometallics* **2000**, *19*, 5546.

Scheme 3. Preparation of *trans* Platinum Metal Chelates **4a,b^a**



^a Conditions: (i) $(PPh_3)_2Pt(C_2H_4)$ (**3**), toluene, 25 °C.

Synthesis of $[\eta^2-(Phosphino-*o*-carboranyl)silyl]-metal$ Complexes $(Cab^{P,Si})_2M$ ($Cab^{P,Si} = \eta^2-(PR_2)(SiMe_2)C_2B_{10}H_{10}-P,Si$; M = Pt (4**, **5**), Pd (**7**, **8**)).** Metal chelates with $\eta^2-[(PR_2)(SiMe_2)C_2B_{10}H_{10}-P,Si]$ were synthesized using the reaction of coordinatively unsaturated metal complexes with the (phosphinoalkyl)silanes **2** via coordination of the phosphine moiety and the oxidative addition of the Si-H bond. When 2 equiv of the (phosphinoalkyl)silanes **2a,b** was treated with 1 equiv of $(PPh_3)_2Pt(C_2H_4)$ (**3**) in toluene at 25 °C, an immediate color change from pale yellow to deep yellow occurred (Scheme 3).

Standard workup and crystallization from toluene-pentane gave $(Cab^{P,Si})_2Pt$ (**4a,b**) in 73–76% yield as a yellow, crystalline solid which was stable in air and stable during brief heating to 100–110 °C. The unusual thermal stability of **4a,b** may be related to the advantageous properties of the *o*-carboranyl unit, including both its electronic and steric effects. Compounds **4a,b** were soluble in toluene, THF, and chloroform and were characterized using 1H , ^{13}C , and ^{31}P NMR and elemental analysis. A *trans* arrangement of the (phosphinoalkyl)silyl ligands in a typical square-planar Pt(II) environment is proposed here on the basis of the $^1J_{Pt-P}$ values, which are in the range 2702–4049 Hz for **4a,b**.⁷ In particular, the 1H NMR chemical shift of δ 1.87 for **4a** as distorted triplets ($^2J_{H-P} = 3$ Hz) resembles the values reported for the typical virtual coupling in *trans*- $Pt(PMe_2R)_2X_2$ (R = Me, Ph) complexes.⁸ This conclusion was substantiated for complex **4a** by using a single-crystal X-ray study. This molecule has a square-planar coordination around the Pt center with two mutually *trans* $SiMe_2-$ units, as shown in Figure 1. The Pt-Si bond is elongated (2.408(1) Å) by the large influence of the $SiMe_2$ ligand in the *trans* position. The reaction in Scheme 2 proceeds with high stereoselectivity, resulting preferentially in the formation of the *trans* isomer. This is unusual, as the chelate-assisted oxidative addition of (phosphinoalkyl)silanes with d^{10} metal complexes usually occurs with *cis* stereochemistry^{3b,d} due to the

(7) (a) Kalt, D.; Schubert, U. *Inorg. Chim. Acta* **2000**, *306*, 211. (b) Kim, Y.-J.; Park, J.-I.; Lee, S.-C.; Osakada, K.; Tanabe, M.; Choi, J.-C.; Koizumi, T.-A.; Yamamoto, T. *Organometallics* **1999**, *18*, 1349.

(8) (a) Yamashita, H.; Tanaka, M.; Goto, M. *Organometallics* **1997**, *16*, 4696. (b) Rieger, A. L.; Carpenter, G. B.; Rieger, P. H. *Organometallics* **1993**, *12*, 842. (c) Brown, M. P.; Puddephatt, R. J.; Upton, C. E. *J. Chem. Soc., Dalton Trans.* **1974**, 2457. (d) Duddel, D. A.; Evans, J. G.; Goggin, P. L.; Goodfellow, R. J.; Rest, A. J.; Smith, J. G. *J. Chem. Soc. A* **1969**, 2134.

Table 1. NMR Spectroscopic Data (δ) for Compounds **2**, **4**, **5**, **8**, **10**, and **12**^a

compd	¹ H	¹³ C	³¹ P
2a	0.37 (d, 6H, SiMe ₂ , ² J _{Si-H} = 4 Hz) 1.26 (d, 6H, PMe ₂ , ² J _{P-H} = 5 Hz) 4.32 (m, 1H, SiH)	-2.25 (d, SiMe ₂ , ¹ J _{Si-C} = 8 Hz) 15.37 (d, PMe ₂ , ¹ J _{P-C} = 17 Hz)	-11.56 (PMe ₂)
2b	0.37 (dd, 6H, SiMe ₂ , ² J _{Si-H} = 4 Hz, ³ J _{H-H} = 1 Hz) 1.31 (t, 6H, POCH ₂ Me, ³ J _{H-H} = 7 Hz) 3.98 (q, 4H, POCH ₂ Me) 4.31 (m, 1H, SiH)	-2.20 (d, SiMe ₂ , ¹ J _{Si-C} = 7 Hz) 16.96 (d, PMe ₂ , ³ J _{P-C} = 9 Hz) 64.64 (d, POCH ₂ , ² J _{P-C} = 31 Hz)	-91.97 (P(OCH ₂ Me) ₂)
2c	0.42 (d, 6H, SiMe ₂ , ² J _{Si-H} = 6 Hz) 4.50 (m, 1H, SiH)	-2.13 (d, SiMe ₂ , ¹ J _{Si-C} = 10 Hz) 128.70, 129.12, 131.00, 131.41, 132.92, 133.17, 134.93, 135.07, 135.45, 135.59, 135.82 (PPh)	17.46 (PPh ₂)
4a	0.33 (d, 12H, SiMe ₂ , ³ J _{Pt-H} = 13 Hz) 1.87 (dt, 12H, PMe ₂ , ³ J _{Pt-H} = 35 Hz, ³ J _{P-H} = 3 Hz)	6.43 (d, SiMe ₂ , ² J _{Pt-C} = 44 Hz) 18.09 (d, PMe ₂ , ² J _{Pt-C} = 39 Hz)	48.60 (d, PMe ₂ , ¹ J _{Pt-P} = 2702 Hz)
4b	0.40 (d, 12H, SiMe ₂ , ³ J _{Pt-H} = 13 Hz)	6.53 (SiMe ₂)	164.80 (d, P(OCH ₂ Me) ₂ , ¹ J _{Pt-P} = 4049 Hz)
5a	1.38 (t, 12H, P(OCH ₂ Me) ₂ , ³ J _{H-H} = 7 Hz) 4.19 (m, 8H, P(OCH ₂ Me) ₂) 0.41 (dd, 12H, SiMe ₂ , ³ J _{Pt-H} = 27 Hz, ² J _{Si-H} = 2 Hz) 1.72 (dd, 12H, PMe ₂ , ³ J _{Pt-H} = 17 Hz, ² J _{P-H} = 7 Hz)	16.29 (P(OCH ₂ Me) ₂) 66.73 (P(OCH ₂ Me) ₂) 1.99 (d, SiMe ₂ , ² J _{Pt-C} = 229 Hz) 19.00 (PMe ₂)	55.05 (d, PMe ₂ , ¹ J _{Pt-P} = 1626 Hz)
5b	0.41 (dd, 12H, SiMe ₂ , ³ J _{Pt-H} = 27 Hz, ² J _{Si-H} = 2 Hz) 1.36 (t, 12H, P(OCH ₂ Me) ₂ , ³ J _{H-H} = 7 Hz), 4.11 (m, 8H, P(OCH ₂ Me) ₂)	1.96 (SiMe ₂) 25.82 (P(OCH ₂ Me) ₂) 47.85 (P(OCH ₂ Me) ₂)	-71.50 (d, P(OCH ₂ Me) ₂ , ¹ J _{Pt-P} = 2492 Hz)
5c	0.56 (dd, 12H, SiMe ₂ , ³ J _{Pt-H} = 28 Hz, ² J _{Si-H} = 2 Hz) 7.12, 7.38 (m, 20H, PPh ₂)	6.56 (d, SiMe ₂ , ² J _{Pt-C} = 111 Hz) 128.03, 128.17, 128.52, 131.79, 134.86 (PPh ₂)	70.99 (d, PPh ₂ , ¹ J _{Pt-P} = 1814 Hz)
8a	0.41 (d, 12H, SiMe ₂ , ² J _{Si-H} = 2 Hz) 1.60 (d, 12H, PMe ₂ , ² J _{P-H} = 5 Hz)	5.72 (SiMe ₂) 21.62 (PMe ₂)	41.68 (PMe ₂)
8b	0.35 (s, 12H, SiMe ₂) 1.38 (t, 12H, P(OCH ₂ Me) ₂ , ³ J _{H-H} = 7 Hz) 4.10 (m, 8H, P(OCH ₂ Me) ₂)	5.40 (SiMe ₂) 16.42 (P(OCH ₂ Me) ₂), 66.58 (P(OCH ₂ Me) ₂)	171.26 (P(OCH ₂ Me) ₂)
8c	0.52 (s, 12H, SiMe ₂) 7.13, 7.35 (m, 20H, PPh ₂)	6.32 (SiMe ₂) 128.13, 128.20, 128.27, 131.56, 134.51, 134.62, 134.72 (PPh ₂)	62.37 (PPh ₂)
10a	-0.75 (ddd, 1H, PtH, ¹ J _{Pt-H} = 1119 Hz, ² J _{P-H(trans)} = 164 Hz, ² J _{P-H(cis)} = 22 Hz) 0.62 (d, 6H, SiMe ₂ , ³ J _{Pt-H} = 32 Hz) 7.11, 7.14, 7.32, 7.78 (m, 25H, PPh)	7.31 (dd, SiMe ₂ , ² J _{Pt-C} = 107 Hz, ¹ J _{Si-C} = 6 Hz) 127.71, 128.16, 129.89, 131.38, 133.96, 135.76 (m, PPh)	34.65 (d, PPh ₃ , ¹ J _{Pt-P} = 1747 Hz) 80.99 (d, PPh ₂ , ¹ J _{Pt-P} = 2660 Hz)
10b	-1.33 (ddd, 1H, PtH, ¹ J _{Pt-H} = 1122 Hz, ² J _{P-H(trans)} = 156 Hz, ² J _{P-H(cis)} = 20 Hz) 0.65 (d, 6H, SiMe ₂ , ³ J _{Pt-H} = 32 Hz, ² J _{Si-H} = 2 Hz) 4.78 (s, 1H, CH _{Cab}) 7.04, 7.36, 7.60 (m, 20H, PPh)	7.07 (dd, SiMe ₂ , ² J _{Pt-C} = 106 Hz, ¹ J _{Si-C} = 7 Hz) 127.91, 131.60, 134.97, 135.17, 135.24, 135.43 (m, PPh)	64.32 (d, (Cab)PPh ₂ , ¹ J _{Pt-P} = 1756 Hz) 77.27 (d, PPh ₃ , ¹ J _{Pt-P} = 2744 Hz)
12a	0.60 (s, 12H, SiMe ₂) 1.27 (d, 12H, PMe ₂ , ² J _{P-H} = 5 Hz)	2.87 (SiMe ₂) 15.54 (PMe ₂)	-17.60 (PMe ₂)
12b	0.65 (s, 12H, SiMe ₂) 1.41 (t, 12H, P(OCH ₂ Me) ₂ , ³ J _{H-H} = 7 Hz) 4.10 (m, 8H, P(OCH ₂ Me) ₂)	5.40 (SiMe ₂) 16.42 (P(OCH ₂ Me) ₂) 66.58 (P(OCH ₂ Me) ₂)	-88.45 (P(OCH ₂ Me) ₂)
12c	0.72 (s, 12H, SiMe ₂) 7.40, 7.42, 7.47, 7.49, 7.69, 7.72, 7.75, 7.79 (20H, PPh ₂)	2.13 (SiMe ₂) 128.77, 129.21, 130.59, 131.11, 133.71, 133.88, 134.68, 135.01, 135.50 (PPh ₂)	11.50 (PPh ₂)

^a CDCl₃ was used as the solvent, and the chemical shifts are reported relative to the residual H of the solvent.

strong *trans* influence of the silyl group. The increased stability of the *trans* products **4a,b** is most likely a consequence of the formation of the two bis(chelate) rings imposed by the bulky *o*-carborane backbones.

Initial attempts to isomerize the *trans* isomers were unsuccessful. The dissolution of *trans*-**4a,b** in toluene and heating of the solutions for 1 day at 110 °C resulted in no changes in *trans*-**4a,b**. However, in the presence of dimethyl acetylenedicarboxylate (DMAD) at 110 °C, the *trans* isomers **4a,b** cleanly rearranged to the thermodynamically favored *cis* isomers, *cis*-(Cab^{P,Si})₂-Pt (**5a,b**), within 1 h (Scheme 4).

Interestingly, only the *trans* isomers **4a,b** with activated acetylene such as DMAD can promote the isomerization to the *cis* form, indicating that there are elec-

tronic influences on the course of the reaction. The isomerization of toluene solutions of *trans*-**4a,b** (0.20 mmol) and DMAD (1.0 mmol) at 110 °C for 1 h afforded high yields of *cis*-**5a,b** (92–96%) as colorless solids.

The ¹H and ³¹P{¹H} NMR spectra of *cis*-**5a,b** in CDCl₃ contain signals of their isomers generated in the solution. The spectra were assigned to *cis*-(Cab^{P,Si})₂Pt (**5a,b**) on the basis of a ¹J_{Pt-P} value (1626–2492 Hz) smaller than that exhibited by *trans*-**4a,b** (¹J_{Pt-P} = 2702–4049 Hz) and because of their similarity to those values previously reported for *cis*-Pt(SiR₃)₂(PR'₃)₂ type complexes.⁹ The solution NMR spectral data of the *cis*-**5a,b** complexes are unambiguous and consistent with the *cis* geometry found in the crystal structure of *cis*-**5a**. Figure 2 depicts the molecular structure of **5a**, which has a

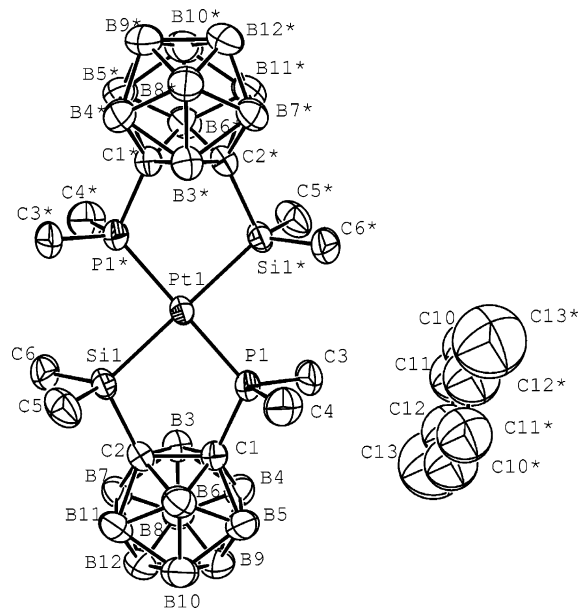


Figure 1. Molecular structure of *trans*-**4a** with thermal ellipsoids drawn at the 30% level.

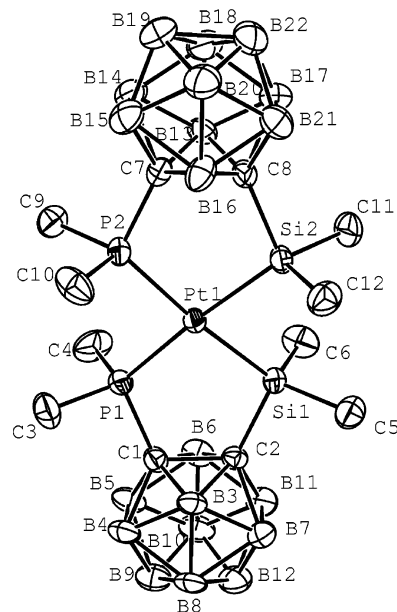
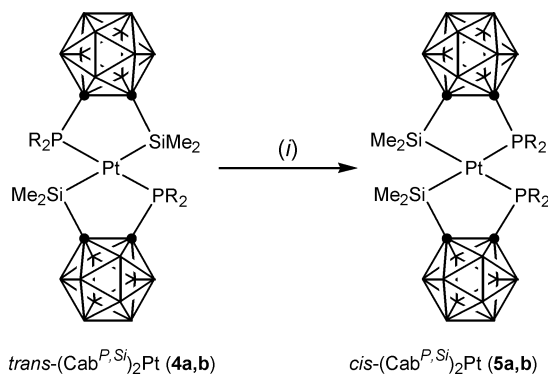


Figure 2. Molecular structure of *cis*-**5a** with thermal ellipsoids drawn at the 30% level.

Scheme 4. Trans to Cis Isomerization of Bis(chelate)platinum Metal Complexes^a



^a Conditions: (i) DMAD, toluene, 110 °C.

distorted-square-planar coordination around the metal center with two dimethylsilyl units in the cis positions. The Pt–P and Pt–Si distances of the terminal ligands and the chelated (phosphino-*o*-carboranyl)silyl ligand do not differ significantly, and the Pt–Si distances are comparable to those found in other Pt(II) silyl complexes.¹⁰

Similar cyclic bis[[(diphenylphosphino)ethyl]diorganosilyl]platinum complexes have been prepared using

the reaction of $\text{Ph}_2\text{PCH}_2\text{CH}_2\text{SiHR}^1\text{R}^2$ ($\text{R}^1, \text{R}^2 = \text{H, Me, Ph}$) with $\text{Pt}(\text{cod})_2$.¹¹ It is well established that the hydrosilylation of low-valent metal complexes by the functional silane $\text{PPh}_2\text{CH}_2\text{CH}_2\text{SiMe}_2\text{H}$ provides access to a family of new bis(chelate) derivatives of the silyl $\text{PPh}_2\text{CH}_2\text{CH}_2\text{SiMe}_2-$, in which the silicon–transition-metal bond is supported by phosphine coordination to the metal.

The isomerization of *cis*-(PhMe_2P)₂Pt(SiMe_2Ph)₂ into *trans*-(PhMe_2P)₂Pt(SiMe_2Ph)₂ catalyzed by di- and oligosilanes has been recently reported.^{7a} In particular, similar *trans*–*cis* isomerization has been observed in the work of Kim et al.^{7b} on *trans*-Pt(SiHPh_2)₂(PMe_3)₂, which is readily converted upon dissolution in THF or CD_2Cl_2 into the thermodynamically more stable *cis* isomer. In contrast, *trans*-**4a,b** are more robust and do not undergo *trans*–*cis* isomerization as readily in solution. The increased stability of the *trans* products **4a,b** is most likely a consequence of the formation of the two bis-chelate rings imposed by the bulky *o*-carborane backbones. In addition, we have used density functional calculations to study both *trans*-**4a** and *cis*-**5a** bis(chelate) platinum complexes and found that the *trans*-**4a** structure is preferred over that of *cis*-**5a** by 1.66 kcal/mol (Figure 3).

Other group 10 metal complexes, such as $\text{Pd}_2(\text{dba})_3$ (**6**) and $\text{Pt}(\text{cod})_2$ (**9**), were tested for the chelate-assisted oxidative addition of **2**, as shown in Schemes 5 and 6 and in Table 2. The reaction of **6** with **2a** results in the bis(chelates) *trans*-($\text{Cab}^{P,Si}$)₂Pd (**7a**) and *cis*-($\text{Cab}^{P,Si}$)₂-Pd (**8a**), in 34% yield with a *trans*:*cis* ratio of 2:1. On the other hand, the reaction of **6** with **2b,c** is *cis*-selective, producing 60–65% yields of *cis*-($\text{Cab}^{P,Si}$)₂Pd (**8b,c**). These results indicate that the stereoselectivity of the reaction is dependent on the electronic and steric characteristics of the ligands around the metal center.

(9) (a) Yamashita, H.; Tanaka, M.; Goto, M. *Organometallics* **1992**, *11*, 3227. (b) Holmes-Smith, R. D.; Stobart, S. R.; Cameron, T. S.; Jochem, K. *J. Chem. Soc., Chem. Commun.* **1981**, 937. (c) Chatt, J.; Eaborn, C.; Ibekwe, S. D.; Kapoor, P. N. *J. Chem. Soc. A* **1970**, 1343.

(10) Recent articles on silylplatinum complexes: (a) Ozawa, F.; Hikida, T. *Organometallics* **1996**, *15*, 4501. (b) Goikhman, R.; Aizenberg, M.; Shimon, L. J. W.; Milstein, D. *J. Am. Chem. Soc.* **1996**, *118*, 10894. (c) Levy, C. J.; Vittal, J. J.; Puddephatt, R. J. *Organometallics* **1996**, *15*, 2108. (d) Levy, C. J.; Puddephatt, R. J.; Vittal, J. J. *Organometallics* **1994**, *13*, 1559. (e) Ozawa, F.; Hikida, T.; Hayashi, T. *J. Am. Chem. Soc.* **1994**, *116*, 2844. (f) Yamashita, H.; Tanaka, M.; Goto, M. *Organometallics* **1993**, *12*, 988. (g) Sakaki, S.; Ieki, M. *J. Am. Chem. Soc.* **1993**, *115*, 2373. (h) Braunstein, P.; Knorr, M.; Hirle, B.; Reinhard, G.; Schubert, U. *Angew. Chem., Int. Ed. Engl.* **1992**, *31*, 1583. (i) Tanaka, M.; Uchimaru, Y.; Lautenschlager, H.-J. *J. Organomet. Chem.* **1992**, *428*, 1. (j) Yamashita, H.; Tanaka, M.; Goto, M. *Organometallics* **1992**, *11*, 3227. (k) Heyn, R. H.; Tilley, T. D. *J. Am. Chem. Soc.* **1992**, *114*, 1917. (l) Grundy, S. L.; Holmes-Smith, R. D.; Stobart, S. R.; Williams, M. A. *Inorg. Chem.* **1991**, *30*, 3333. (m) Pham, E. K.; West, R. *Organometallics* **1990**, *9*, 1517.

(11) (a) Grundy, S. L.; Holmes-Smith, R. D.; Stobart, S. R.; Williams, M. A. *Inorg. Chem.* **1991**, *30*, 3333. (b) Holmes-Smith, R. D.; Stobart, S. R.; Cameron, T. S.; Jochem, K. *J. Chem. Soc., Chem. Commun.* **1981**, 937.

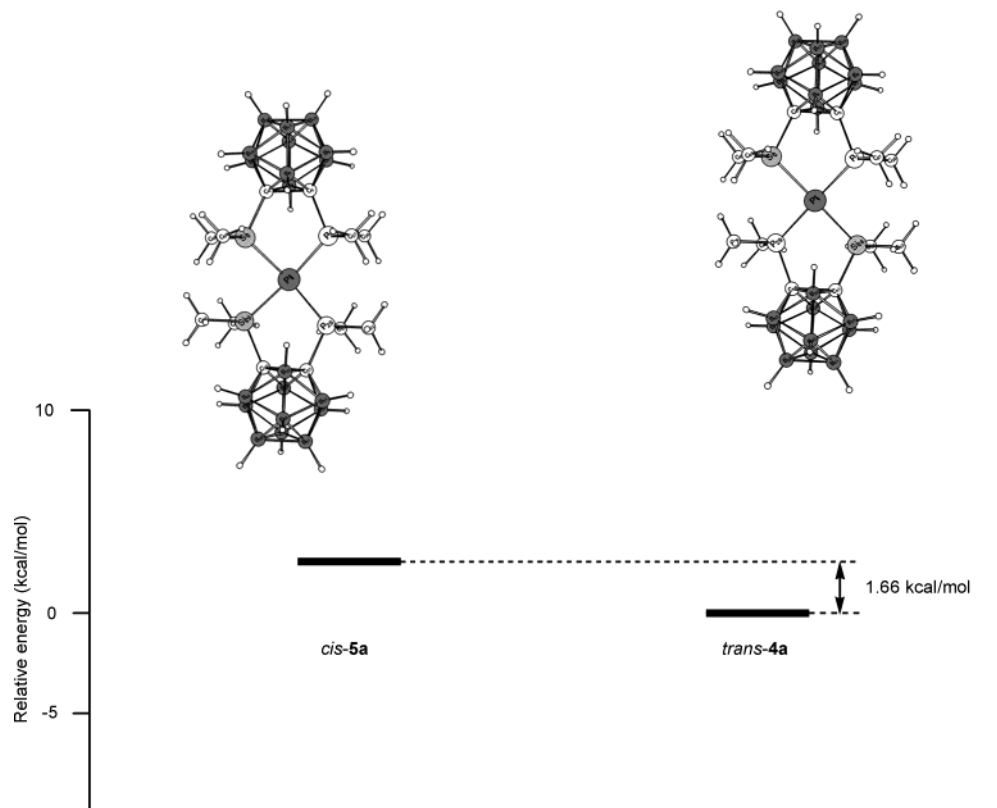
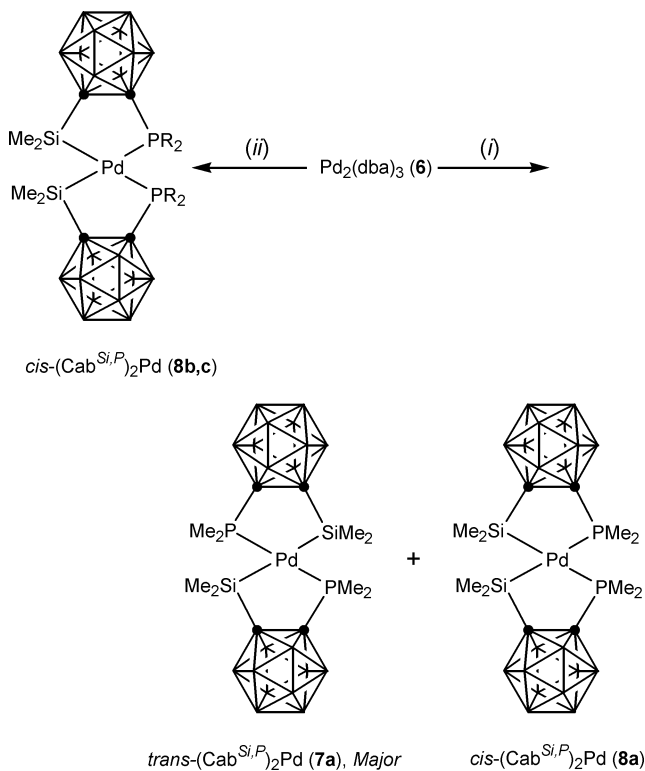


Figure 3. Energy profiles of *trans*-4a and *cis*-5a.

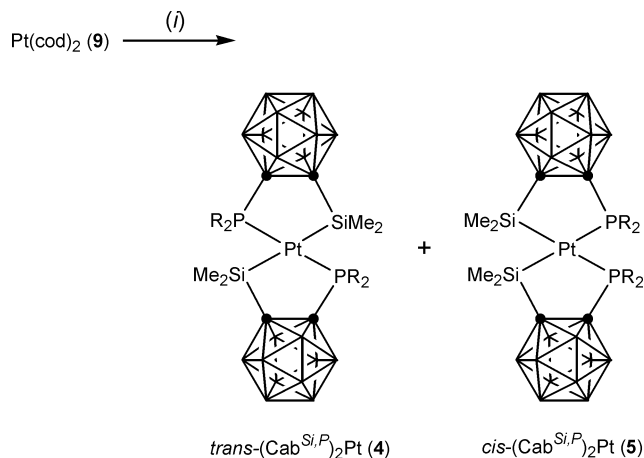
Scheme 5. Reaction of Pd₂(dba)₃ (6) with (Phosphino-*o*-carboranyl)silane (2)^a



^a Conditions: (i) 2 **2a**, toluene, 25 °C; (ii) 2 **2b,c**, toluene, 25 °C.

The ¹H, ¹³C, and ³¹P NMR spectral data for the resulting palladium species *trans*-7 and *cis*-8 are summarized in Table 1. All the complexes exhibit NMR spectra that are in agreement with their proposed

Scheme 6. Reaction of Pt(cod)₂ (9) with (Phosphino-*o*-carboranyl)silane (2)^a



^a Conditions: (i) 2 **2**, toluene, 25 °C.

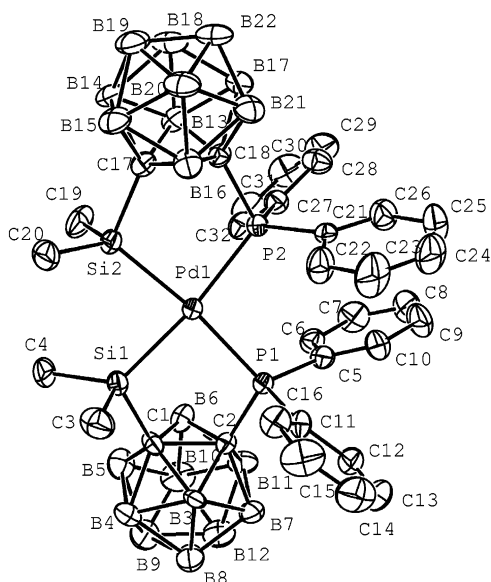
structures. In addition, we established the structure of *cis*-8c unambiguously using single-crystal X-ray analysis, as shown in Figure 4. The crystallographic data and processing parameters are given in Table 3; selected bond distances and angles are given in Tables 4 and 5, respectively. Complex *cis*-8c has a slightly distorted square-planar geometry with a *cis* arrangement of the two silicon atoms. The equatorial plane is defined by the Pd(1), P(1), P(2), Si(1), and Si(2) atoms and is relatively planar with an average atomic displacement of 0.0426 Å. The two five-membered metallacycles (Pd(1), C(1), C(2), Si(1), P(1); Pd(1), C(17), C(18), Si(2), P(2)) are twisted with respect to each other at a dihedral angle of 8.8(1)°. These metallacycles are also twisted with respect to the equatorial plane, with dihedral

Table 2. Chelate-Assisted Oxidative Addition Reaction of 2

$$2 \text{ Me}_2\text{Si}^{\text{H}}\text{PR}_2 \xrightarrow{\text{ML}_n} (\text{Cab}^{\text{Si,P}}) + \text{Me}_2\text{Si}^{\text{H}}\text{M}(\text{PR}_2)_2$$

entry	substrate	ML _n	(Cab ^{Si,P}) ₂ M		yield (%) ^b
			trans	cis	
1	2a	(PPh ₃) ₂ Pt(C ₂ H ₄) (3)	4a	none	73
2	2b	(PPh ₃) ₂ Pt(C ₂ H ₄) (3)	4b	none	76
3	2a	Pd ₂ (dba) ₃ (6)	2 7a^c	1 8a^c	34
4	2b	Pd ₂ (dba) ₃ (6)	none	8b	65
5	2c	Pd ₂ (dba) ₃ (6)	none	8c	60
6	2a	Pt(cod) ₂ (9)	2 4a^c	1 5a^c	59
7	2b	Pt(cod) ₂ (9)	1 4b^c	1 5b^c	51
8	2c	Pt(cod) ₂ (9)	1 4c^c	6 5c^c	43

^a Conditions: 0.60 mmol of **2**, benzene, 25 °C, Ar atm. ^b Yields determined after recrystallization or chromatography. ^c Stereoisomeric ratios were determined by NMR.

**Figure 4.** Molecular structure of *cis*-**8c** with thermal ellipsoids drawn at the 30% level.

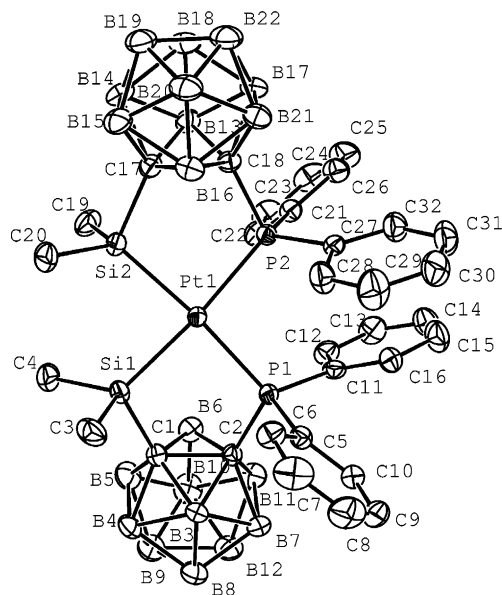
angles of 17.1(1) and 8.4(1)°, respectively. The Pd–Si bond distance (2.358(2)–2.361(2) Å) of *cis*-**8c** is in agreement with the values observed for Pd(SiMe₂CH₂CH₂PPh₂)₂ (2.367(1) Å)¹² and (dcpe)Pd(SiHMe₂)₂ (2.3561 Å)¹³ and for analogous complexes (2.34–2.41 Å).¹⁴ The ¹H, ¹³C, and ³¹P NMR spectra of *cis*-**8c** are consistent with the structure determined by X-ray crystallography. An ¹H NMR signal ascribable to the Pd–SiMe₂ moiety was observed at 0.52 ppm. The ³¹P NMR signal had clearly shifted, moving from a value of 17.46 ppm for **2c** to 62.37 ppm for *cis*-**8c**.

Bis(silyl)palladium complexes have already been reported by Ito et al.¹⁵ and have been implicated as key

(12) Murakami, M.; Yoshida, T.; Ito, Y. *Organometallics* **1994**, *13*, 2900.

(13) Pan, Y.; Mague, J. T.; Fink, M. J. *Organometallics* **1992**, *11*, 3495.

(14) (a) Suginome, M.; Oike, H.; Park, S.; Ito, Y. *Bull. Chem. Soc. Jpn.* **1996**, *69*, 289. (b) Michalczyk, M. J.; Tilley, T. D. *J. Am. Chem. Soc.* **1992**, *114*, 1917. (c) Holmes-Smith, R. D.; Stobart, S. R.; Cameron, T. S.; Jochem, K. *J. Chem. Soc., Chem. Commun.* **1981**, 937.

**Figure 5.** Molecular structure of *cis*-**5c** with thermal ellipsoids drawn at the 30% level.

intermediates in the Pd-catalyzed bis-silylation of alkynes.¹⁶ This suggested that an investigation of the reactivity of *cis*-(Cab^{P,Si})₂Pd (**8b,c**) with alkynes might be useful. However, these *cis* isomers are inactive toward bis-silylation, indicating that the bulky *o*-carborane backbone confers some additional strength to the Pd–Si bond.

In contrast, the route using Pt(cod)₂ (**9**) does not exhibit sufficient stereoselectivity. The use of **2a** gives **4a** and **5a** with a trans:cis ratio of 2:1, whereas **2b** yields **4b** and **5b** with a trans:cis ratio of 1:1. On the other hand, when **9** is reacted with **2c**, the major product formed is the *cis* isomer **5c**, as well as a minor amount of the *trans* isomer **4c**. A *cis* arrangement of the chelated ligands in complex **5c** is indicated by ¹J_{Pt–P} = 1814 Hz, which is close to that reported for *cis*-[Pt(PPh₂CH₂CH₂SiMe₂)₂] (1608 Hz), which has mutually *cis* phosphines.^{3b} This conclusion was corroborated by the results of an X-ray crystal structure determination (Figure 5). The four bulky groups bonded to the platinum atom are accommodated in the square plane by distortion of the bond angles centered at Pt. The Pt–P and Pt–Si distances of the terminal ligands and the chelated (phosphino-*o*-carboranyl)silyl ligand do not differ significantly, and the Pt–Si distances are comparable to those in other Pt(II) silyl complexes.¹⁰

Although a wide range of kinetically stabilized *trans* isomers can be obtained under mild conditions, the stereochemistry of the reaction nevertheless appears to be dependent on which silane and metal complex are employed. For example, changing the alkyl substituent on the phosphorus center of the silane to one that is more electron donating and less sterically demanding, as is the case in **2a**, exclusively leads to the *trans* isomer. Increased stereoselectivity is also found for metal complexes such as **3** and **6**; whether the *trans* or

(15) (a) Murakami, M.; Yoshida, T.; Kawanami, S.; Ito, Y. *J. Am. Chem. Soc.* **1995**, *117*, 6408. (b) Murakami, M.; Yoshida, T.; Ito, Y. *Organometallics* **1994**, *13*, 2900.

(16) (a) Murakami, M.; Suginome, M.; Fujimoto, K.; Ito, Y. *Angew. Chem., Int. Ed. Engl.* **1993**, *32*, 1473. (b) Obora, Y.; Tsuji, Y.; Kawamura, T. *Organometallics* **1993**, *12*, 2853 and references therein.

Table 3. X-ray Crystallographic Data and Processing Parameters for Compounds 4a, 5a,c, 8c, and 10a,c

	4a	5a	5c	8c	10a	10b
formula	B ₁₀ C ₁₉ H ₅₂ Si ₂ -P ₂ Pt	B ₂₀ C ₁₂ H ₄₄ Si ₂ -P ₂ Pt	B ₂₀ C ₃₂ H ₅₂ Si ₂ -P ₂ Pt	B ₂₀ C ₃₂ H ₅₂ Si ₂ -P ₂ Pd	B ₁₀ C ₃₄ H ₄₂ Si ₂ -P ₂ Pt	B ₂₀ C ₃₀ H ₄₈ Si ₂ -P ₂ Pt
fw	810.03	717.88	966.15	877.46	843.90	910.00
cryst class	triclinic	monoclinic	monoclinic	monoclinic	monoclinic	triclinic
space group	<i>P</i> $\bar{1}$	<i>P</i> 2 ₁ / <i>n</i>	<i>P</i> 2 ₁ / <i>c</i>	<i>P</i> 2 ₁ / <i>c</i>	<i>P</i> 2 ₁ / <i>c</i>	<i>P</i> $\bar{1}$
Z	1	4	4	4	4	2
cell constants						
<i>a</i> , Å	8.6548(3)	9.5000(9)	11.8496(8)	11.880 (1)	13.0608(6)	11.9428(6)
<i>b</i> , Å	11.0158(8)	22.673(1)	15.686(2)	15.645 (1)	18.296(1)	12.8016(6)
<i>c</i> , Å	11.0685(7)	14.6629(6)	23.404(1)	23.405 (2)	16.3890(7)	13.681(2)
α , deg	104.516(5)					96.647(8)
β , deg	106.106(4)	90.564(5)	93.792(5)	93.557(7)	103.262(4)	95.711(8)
γ , deg	98.033(4)					92.512(4)
<i>V</i> , Å ³	956.3(1)	3141.8(4)	4340.7(6)	4341.9(6)	3811.9(3)	2064.0(4)
μ , mm ⁻¹	3.830	4.652	3.389	0.583	3.821	3.531
cryst size, mm	0.3 × 0.45 × 0.45	0.2 × 0.2 × 0.3	0.35 × 0.5 × 0.5	0.4 × 0.4 × 0.5	0.3 × 0.3 × 0.3	0.2 × 0.3 × 0.3
<i>d</i> _{calc} , g/cm ³	1.413	1.518	1.478	1.342	1.470	1.464
<i>F</i> (000)	400	1408	1920	1792	1672	900
radiation			Mo K α (λ = 0.7107)			
θ range, deg	1.96–25.97	1.66–25.97	1.56–25.98	1.57–25.97	1.60–25.97	1.51–25.97
<i>h</i> , <i>k</i> , <i>l</i> collected	0–10, +13 to –13, +13 to –13,	0–11, 0–27, –18 to +18	0–14, 0–19, –28 to +28	0–14, 0–19, –28 to +28	–16 to +16, 0–22, 0–20	0–14, 0–15, –16 to +16
no. of rflns measd	4060	6558	8974	8886	7793	8535
no. of unique rflns	3758	6142	8510	8459	7481	8086
no. of rflns used in refinement (<i>I</i> > 2 σ (<i>I</i>))	3709	5079	6676	5760	4919	7320
no. of params	199	362	558	558	471	534
R1 ^a	0.0288	0.0342	0.0298	0.0614	0.0389	0.0311
wR2 ^a	0.0732	0.1539	0.0699	0.2080	0.1143	0.1317
GOF	1.078	1.236	1.076	1.057	0.710	1.116

^a R1 = $\sum F_o - F_c$ (based on reflections with $F_o^2 > 2\sigma F^2$). wR2 = $[\sum [w(F_o^2 - F_c^2)^2] / \sum [w(F_o^2)^2]]^{1/2}$; $w = 1/[\sigma^2(F_o^2) + (0.095P)^2]$; $P = [\max(F_o^2, 0) + 2F_c^2]/3$ (also with $F_o^2 > 2\sigma F^2$).

Table 4. Selected Interatomic Distances (Å) for Compounds 4a, 5a,c, 8c, and 10a,c

Compound 4a									
Pt(1)–P(1)	2.251(1)	Pt(1)–Si(1)	2.408(1)	Pt(1)–P(1)#1	2.251(1)	Pt(1)–Si(1)#1	2.408(1)	P(1)–C(3)	1.813(5)
P(1)–C(4)	1.824(5)	P(1)–C(1)	1.869(4)	P(1)–C(4)	1.824(5)	Si(1)–C(5)	1.878(5)	Si(1)–C(6)	1.888(5)
Si(1)–C(2)	1.950(4)	C(1)–C(2)	1.676(6)	C(10)–C(11)	1.23(2)	C(11)–C(12)	1.34(2)	C(12)–C(13)	1.17(3)
C(10)–C(12)#2	1.42(2)	C(12)–C(10)#2	1.42(2)						
Compound 5a									
Pt(1)–P(1)	2.3122(2)	Pt(1)–P(2)	2.3085(2)	Pt(1)–Si(1)	2.3492(2)	Pt(1)–Si(2)	2.3532(2)	P(1)–C(3)	1.811(9)
P(1)–C(4)	1.818(9)	P(1)–C(1)	1.884(8)	P(2)–C(9)	1.785(8)	P(2)–C(10)	1.817(9)	P(2)–C(7)	1.851(8)
Si(1)–C(5)	1.874(8)	Si(1)–C(6)	1.886(9)	Si(1)–C(2)	1.928(7)	Si(2)–C(11)	1.859(9)	Si(2)–C(12)	1.866(9)
Si(2)–C(8)	1.947(7)	C(1)–C(2)	1.667(1)						
Compound 5c									
Pt(1)–P(1)	2.338(1)	Pt(1)–Si(1)	2.362(1)	Pt(1)–P(2)	2.337(1)	Pt(1)–Si(2)	2.361(1)	Si(1)–C(1)	1.953(5)
P(1)–C(2)	1.887(4)	Si(2)–C(17)	1.950(5)	P(2)–C(18)	1.882(4)	Si(1)–C(3)	1.871(5)	Si(1)–C(4)	1.889(5)
P(1)–C(5)	1.812(4)	P(1)–C(11)	1.825(4)	Si(2)–C(19)	1.879(5)	Si(2)–C(20)	1.882(5)	P(2)–C(21)	1.823(4)
P(2)–C(27)	1.829(4)								
Compound 8c									
Pd(1)–P(1)	2.363(2)	Pd(1)–Si(1)	2.361(2)	Pd(1)–P(2)	2.357(2)	Pd(1)–Si(2)	2.358(2)	Si(1)–C(1)	1.959(7)
P(1)–C(2)	1.890(7)	Si(2)–C(17)	1.951(8)	P(2)–C(18)	1.881(7)	Si(1)–C(3)	1.875(9)	Si(1)–C(4)	1.887(8)
P(1)–C(5)	1.814(7)	P(1)–C(11)	1.821(7)	Si(2)–C(19)	1.889(8)	Si(2)–C(20)	1.874(8)	P(2)–C(21)	1.822(7)
P(2)–C(27)	1.832(8)								
Compound 10a									
Pt(1)–P(1)	2.271(2)	Pt(1)–Si(1)	2.307(2)	Pt(1)–P(2)	2.353(2)	P(1)–C(3)	1.808(6)	P(1)–C(9)	1.832(6)
P(1)–C(1)	1.907(6)	P(2)–C(17)	1.823(6)	P(2)–C(23)	1.830(6)	P(2)–C(29)	1.837(6)	Si(1)–C(16)	1.861(2)
Si(1)–C(15)	1.875(2)	Si(1)–C(2)	1.942(7)						
Compound 10b									
Pt(1)–P(1)	2.2804(1)	Pt(1)–Si(1)	2.3228(2)	Pt(1)–P(2)	2.3642(1)	P(1)–C(3)	1.822(6)	P(1)–C(9)	1.824(6)
P(1)–C(1)	1.864(6)	P(2)–C(19)	1.826(6)	P(2)–C(25)	1.837(7)	P(2)–C(17)	1.896(6)	Si(1)–C(16)	1.877(9)
Si(1)–C(15)	1.877(1)	Si(1)–C(2)	1.941(7)						

the *cis* isomer is produced depends on the steric bulk of the phosphine substituent.

Of the silanes we studied, **2c** failed to produce an appreciable amount of *trans*-bis(chelates). Interestingly, **3** reacted with **2c** by displacement of the ethylene ligand and the oxidative addition of the Si–H bond¹⁷ to generate the chelating (phosphinoalkyl)silane stabilized

cis-[(hydridosilyl)Pt^{II}] complex¹⁸ (Cab^{*P,Si*})Pt(H)(PPh₃) (**10a**). In contrast, such a hydridosilyl mono(chelate) was

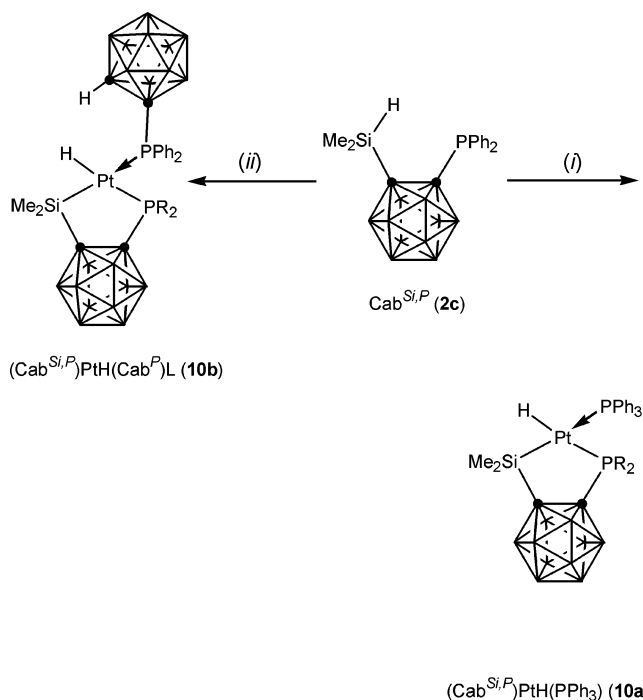
(17) (a) Schubert, U. In *Progress in Organosilicon Chemistry*; Marciniak, B., Chojnowski, J., Eds.; Gordon and Breach: Lausanne, Switzerland, 1995; pp 287–307. (b) Sakaki, S.; Ieki, M. *J. Am. Chem. Soc.* **1993**, *115*, 2373. (c) Schubert, U. *Adv. Organomet. Chem.* **1990**, *30*, 151.

Table 5. Selected Interatomic Angles (deg) for Compounds 4a, 5a,c, 8c, and 10a,c

Compound 4a									
P(1)–Pt(1)–P(1)#1	180.0	P(1)#1–Pt(1)–Si(1)	92.12(4)	P(1)#1–Pt(1)–Si(1)#1	87.88(4)	C(3)–P(1)–C(4)	103.9(3)		
C(4)–P(1)–C(1)	104.2(2)	C(4)–P(1)–Pt(1)	113.9(2)	C(6)–Si(1)–Pt(1)	117.6(2)	P(1)–Pt(1)–Si(1)	87.88(4)	C(3)–P(1)–Pt(1)	118.5(2)
P(1)–Pt(1)–Si(1)#1	92.12(4)	Si(1)–Pt(1)–Si(1)#1	180.0	C(3)–P(1)–C(1)	101.2(2)				
C(1)–P(1)–Pt(1)	113.3(1)	C(5)–Si(1)–Pt(1)	118.9(2)	C(2)–Si(1)–Pt(1)	106.54(1)				
Compound 5a									
P(2)–Pt(1)–P(1)	97.36(7)	P(2)–Pt(1)–Si(1)	175.11(7)	P(1)–Pt(1)–Si(1)	87.03(7)	P(2)–Pt(1)–Si(2)	87.97(7)		
P(1)–Pt(1)–Si(2)	174.57(7)	Si(1)–Pt(1)–Si(2)	87.61(7)	C(3)–P(1)–C(4)	104.0(5)	C(3)–P(1)–C(1)	101.0(4)		
C(4)–P(1)–C(1)	104.1(4)	C(3)–P(1)–Pt(1)	118.7(4)	C(4)–P(1)–Pt(1)	114.9(4)	C(1)–P(1)–Pt(1)	112.3(2)		
C(9)–P(2)–C(10)	102.3(5)	C(9)–P(2)–C(7)	101.7(4)	C(10)–P(2)–C(7)	105.3(4)	C(9)–P(2)–Pt(1)	118.5(3)		
C(10)–P(2)–Pt(1)	115.8(3)	C(7)–P(2)–Pt(1)	111.5(2)	C(5)–Si(1)–Pt(1)	122.2(3)	C(6)–Si(1)–Pt(1)	113.2(3)		
C(2)–Si(1)–Pt(1)	106.9(2)	C(11)–Si(2)–Pt(1)	119.3(3)	C(12)–Si(2)–Pt(1)	115.8(3)	C(8)–Si(2)–Pt(1)	108.1(2)		
Compound 5c									
P(1)–Pt(1)–Si(1)	87.51(4)	Si(2)–Pt(1)–Si(1)	86.69(4)	P(2)–Pt(1)–Si(2)	87.76(4)	P(2)–Pt(1)–P(1)	98.00(4)		
C(2)–P(1)–Pt(1)	110.1(1)	C(1)–C(2)–P(1)	112.1(3)	C(2)–C(1)–Si(1)	116.1(3)	C(1)–Si(1)–Pt(1)	105.9(1)		
C(18)–C(17)–Si(2)	116.2(3)	C(17)–Si(2)–Pt(1)	107.6(1)	C(17)–C(18)–P(2)	112.4(3)	C(18)–P(2)–Pt(1)	112.1(1)		
C(5)–P(1)–C(11)	104.7(2)	C(21)–P(2)–C(27)	111.5(2)						
Compound 8c									
P(1)–Pd(1)–Si(1)	88.08(7)	Si(1)–Pd(1)–Si(2)	84.71(7)	Si(2)–Pd(1)–P(2)	88.01(7)	P(1)–Pd(1)–P(2)	99.11(6)		
Pd(1)–P(1)–C(2)	109.9(2)	P(1)–C(2)–C(1)	111.5(4)	C(2)–C(1)–Si(1)	117.6(4)	C(1)–Si(1)–Pd(1)	105.1(2)		
Si(2)–C(17)–C(18)	117.2(4)	Pd(1)–Si(2)–C(17)	107.0(2)	C(17)–C(18)–P(2)	112.1(4)	C(18)–P(2)–Pd(1)	111.8(2)		
C(5)–P(1)–C(11)	104.2(3)	C(21)–P(2)–C(27)	110.8(3)						
Compound 10a									
P(1)–Pt(1)–Si(1)	90.91(7)	P(1)–Pt(1)–P(2)	105.18(5)	Si(1)–Pt(1)–P(2)	163.81(7)	C(3)–P(1)–C(9)	105.6(3)		
C(3)–P(1)–C(1)	101.7(3)	C(9)–P(1)–C(1)	105.3(3)	C(3)–P(1)–Pt(1)	114.4(2)	C(9)–P(1)–Pt(1)	117.6(2)		
C(1)–P(1)–Pt(1)	110.7(2)	C(17)–P(2)–C(23)	105.4(3)	C(17)–P(2)–Pt(1)	111.7(2)	C(23)–P(2)–Pt(1)	117.2(2)		
C(29)–P(2)–Pt(1)	116.0(2)	C(16)–Si(1)–Pt(1)	114.8(4)	C(15)–Si(1)–Pt(1)	116.3(4)	C(2)–Si(1)–Pt(1)	107.7(2)		
Compound 10b									
P(1)–Pt(1)–Si(1)	91.16(6)	P(1)–Pt(1)–P(2)	99.34(5)	Si(1)–Pt(1)–P(2)	163.46(7)	C(3)–P(1)–C(9)	110.2(3)		
C(3)–P(1)–C(1)	104.7(3)	C(9)–P(1)–C(1)	101.6(2)	C(3)–P(1)–Pt(1)	112.30(2)	C(9)–P(1)–Pt(1)	116.46(2)		
C(1)–P(1)–Pt(1)	110.43(2)	C(19)–P(2)–C(25)	107.8(3)	C(16)–Si(1)–Pt(1)	110.7(4)	C(25)–P(2)–C(17)	104.3(3)		
C(19)–P(2)–Pt(1)	116.0(2)	C(25)–P(2)–Pt(1)	107.4(2)	C(17)–P(2)–Pt(1)	117.56(2)	C(15)–Si(1)–Pt(1)	121.2(4)		
C(2)–Si(1)–Pt(1)	106.82(2)								

not observed for the oxidative addition of analogous (phosphinoalkyl)silanes.³ Thus, as can be seen in Scheme 7, an increase in the steric bulk of the phosphine substituent appears to retard the second oxidative addition, as manifested in the higher yields obtained for **10a**. Given this steric constraint, we next turned to determining whether high yields of the mono(chelate) could be obtained if **2c** was reacted with **9** in the presence of the bulky ancillary *o*-carboranylphosphine ligand (Cab)PPh₂. Indeed, **2c** was found to cleanly react with **9** and (Cab)PPh₂ to provide the sterically encumbered *cis*-[(hydridosilyl)Pt^{II}] complex (Cab^{Si,P})Pt(H)-[(Cab)PPh₂] (**10b**), which is stable well above 100 °C. The structures of **10a,b** agree with the conclusions from the solution NMR data that the atoms are arranged in a square-pyramidal framework. The hydride ligand was not located by X-ray diffraction; however, its presence was confirmed by the appearance of its ¹H NMR resonance at around δ –1 (¹J_{PtH} ≈ 1119 Hz).

Figure 6 shows the structure of **10a** as determined by X-ray crystallography. The coordination geometry around the Pt center of the complexes can be rationalized as a distorted square plane containing two PPh₂R (R = Ph, *o*-carborane) ligands at mutually *cis* positions and a dimethylsilyl unit and a hydrido ligand coordinated to the Pt(II) center. The Pt–Si bond distances (2.307(2) Å) are in the range previously reported for

Scheme 7. Preparation of *cis*-[(hydridosilyl)Pt^{II}] Complexes 10a,b^a

^a Conditions: (i) (PPh₃)₂Pt(C₂H₄) (**3**), toluene, 25 °C; (ii) Pt(cod)₂ (**9**), (Cab)PPh₂, toluene, 25 °C.

silylplatinum complexes (2.34–2.40 Å).¹⁰ The Pt(1)–P(2) bond (2.353(2) Å) is longer than the Pt(1)–P(1) bond (2.271(2) Å), indicating that the trans influence of the dimethylsilyl ligand is more significant than that of the

(18) (a) Mullica, D. F.; Sappenfield, E. L.; Hampden-Smith, M. J. *Polyhedron* **1991**, *10*, 867. (b) Clark, H. C.; Hampden-Smith, M. J. *Coord. Chem. Rev.* **1987**, *79*, 229. (c) Clark, H. C.; Hampden-Smith, M. J. *J. Am. Chem. Soc.* **1986**, *108*, 3829. (d) Azizian, H.; Dixon, K. R.; Eaborn, C.; Pidcock, A.; Shuaib, N. M.; Vinaixa, J. *J. Chem. Soc., Chem. Commun.* **1982**, 1020.

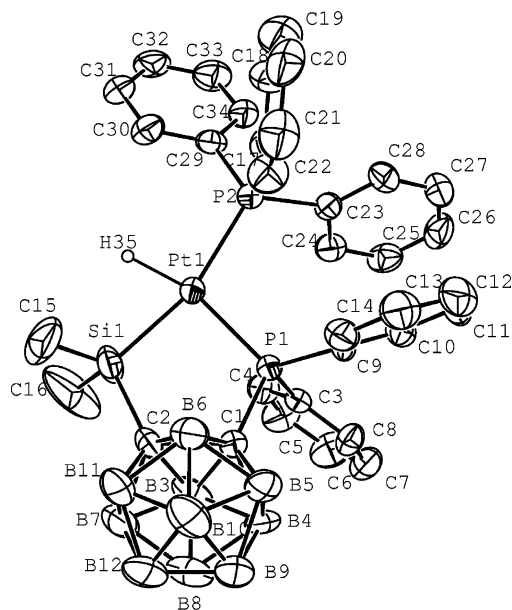


Figure 6. Molecular structure of **10a** with thermal ellipsoids drawn at the 30% level.

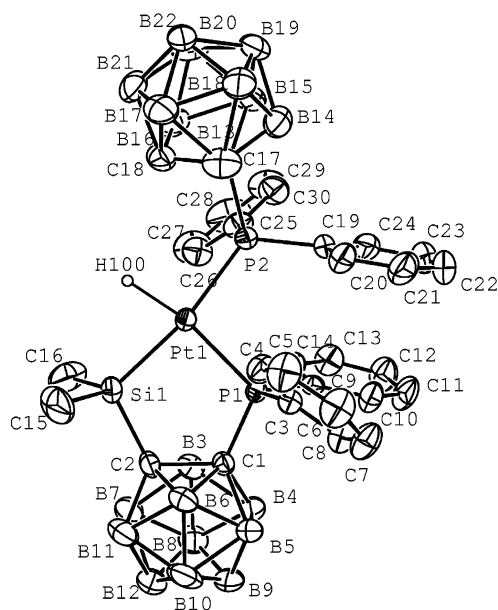


Figure 7. Molecular structure of **10b** with thermal ellipsoids drawn at the 30% level.

hydride. An analogous PPh_3 -coordinated complex, *cis*-[Pt(H)(SiPh₃)(PPh₃)₂], also has dissimilar Pt–P bonds (2.332(2) and 2.298(3) Å), which arises because the *trans* influence of the SiPh₃ ligand is greater than that of the hydride.¹⁹ Serious deviation of the bond angles around the metal center from the ideal 90 or 180° can be attributed to the more severe steric repulsion between the silyl and phosphine ligands than exists between the hydride and other ligands.

A similar distorted-square-planar arrangement about the platinum atom is found in (*Cab*^{*P,Si*})Pt(H)[(PPh₂)–C₂B₁₀H₁₁] (**10b**) (Figure 7). The platinum atom is bonded to a hydrogen atom, two phosphorus atoms, and a silicon atom. The atoms of the first platinum coordination sphere display major deviations from planarity (mean

deviation of –1.004(2) Å), probably as a result of the maximal space requirement for the bulky *o*-carboranyl phosphine ligand. It has been established that the greater *trans* influence of the dimethylsilyl group compared with that of the hydride means that the Pt(1)–P(2) bond is longer than the Pt(1)–P(1) bond.¹⁹ The measured Pt(1)–Si(1) distance is comparable to other previously published values.¹⁰

The ¹H NMR spectrum of **10a** contains a signal due to the hydride ligand at δ –0.75 as a doublet of doublets flanked with satellites caused by the ¹⁹⁵Pt metal center (¹*J*_{Pt–H} = 1119 Hz). The large difference between the two ²*J*_{P–H} values (164 and 22 Hz) indicates that the phosphine ligands occupy mutually *cis* positions. The ³¹P{¹H} NMR spectrum contains signals at δ 80.99 and 34.65 with ¹*J*_{Pt–P} values of 2660 and 1747 Hz, respectively. The latter is assigned to the phosphine ligand at the *trans* position of the dimethylsilyl ligands on the basis of a comparison of the ¹*J* values with those of already reported silylplatinum complexes.¹⁰ This assignment is consistent with the relative magnitude of the *trans* influence of SiMe₃ and H ligands observed in the crystallographic results. Complex **10b** gives rise to similar NMR spectra. Although several *cis*-Pt(H)(SiAr₃)(PPh₃)₂ type complexes have already been prepared from the reaction of HSiAr₃ with Pt(PPh₃)₄ and with **3**,^{19,20} there have been no reports of similar *P,Si*-chelate complexes. The preferential *cis* configuration of **10a,b** can be attributed to the fact that the *trans* influence of both the dimethylsilyl and hydride ligands is much greater than that of PPh₃, rendering the *trans* structure unstable.

Preparation of the Linear Bis(phosphino)disilane 1,2-Bis(1-PR₂-*o*-carboranyl)-1,1,2,2-tetramethyl-1,2-disilane (R = Me (12a**), OEt (**12b**), Ph (**12c**)).** The bis(phosphino)disilanes (**12**) were readily prepared from the dilithium salt of the bis(*o*-carboranyl)disilanes (**11**) with 2 equiv of PR₂Cl (R = Me (**a**), OEt (**b**), Ph (**c**)). The dilithium salt of bis(*o*-carboranyl)disilane generated by the reaction of *n*-BuLi with bis(*o*-carboranyl)disilane (**11**) was reacted with dialkylchlorophosphine to give the bis(phosphino)disilanes (**12**) in 62–70% yield (Scheme 8). The colorless products **12** were crystalline solids that were relatively stable in air and during brief heating to 110–120 °C. The compounds **12** were readily soluble in hexane, toluene, and THF. The ¹H, ¹³C, and ²⁹Si NMR spectra and the elemental analysis of **12** were found to be consistent with the proposed structures. The ²⁹Si NMR chemical shift of –7.2 to –9.0 ppm was shifted downfield from –3.29 ppm for **12a–c**.

Reaction of **12 with the Palladium Complex Pd₂(dba)₃ (**6**).** Treatment of the disilanes **12** with Pd₂(dba)₃ (**6**) in toluene at room temperature for 30 min resulted in the oxidative addition of the Si–Si bond²¹ to the palladium center to form the *cis*-bis(chelate) palladium complexes **8** (Scheme 9).

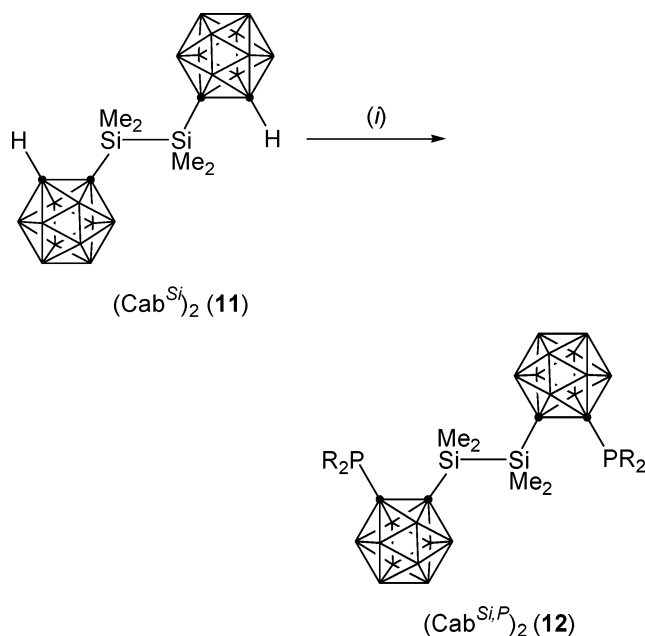
The composition and stereochemistry of **8** were elucidated from their ³¹P, ¹H, and ¹³C NMR spectra and

(20) Azizian, H.; Dixon, K. R.; Eaborn, C.; Pidcock, A.; Shuaib, N. M.; Vinaixa, J. *J. Chem. Soc., Chem. Commun.* **1982**, 1020.

(21) (a) Ozawa, F.; Sugawara, M.; Hayashi, T. *Organometallics* **1994**, *13*, 3237. (b) Murakami, M.; Yoshida, T.; Ito, Y. *Organometallics* **1994**, *13*, 2900. (c) Pan, Y.; Mague, J. T.; Fink, M. J. *Organometallics* **1992**, *11*, 3495. (d) Michalczyk, M. J.; Recatto, C. A.; Calabrese, J. C.; Fink, M. J. *J. Am. Chem. Soc.* **1992**, *114*, 7955. (e) Heyn, R. H.; Tilley, T. D. *J. Am. Chem. Soc.* **1992**, *114*, 1917 and references therein.

(19) Latif, L. A.; Eaborn, C.; Pidcock, A. P.; Weng, N. S. *J. Organomet. Chem.* **1994**, *474*, 217.

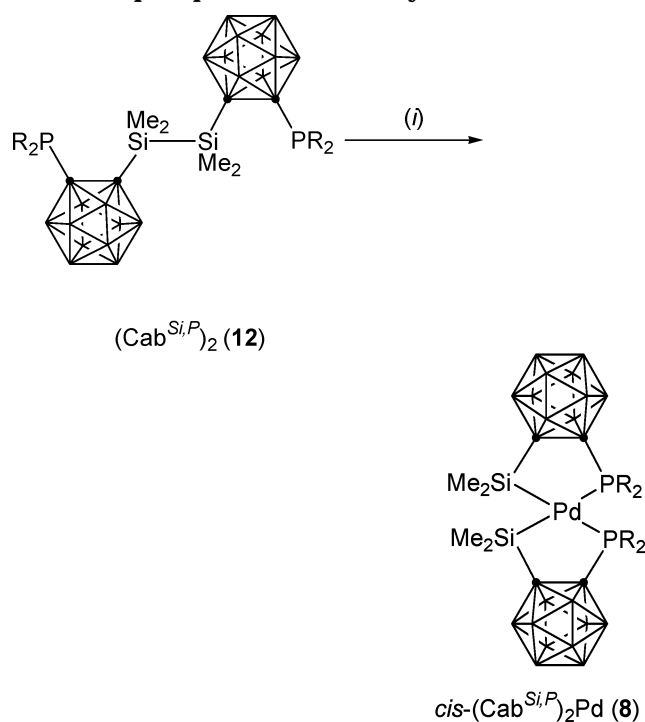
Scheme 8. Synthesis of Bis(phosphino-*o*-carboranyl)disilane **12^a**



R = Me **12a**; OEt **12b**; Ph **12c**

^a Conditions: (i) 2 BuⁿLi, THF, -78 °C; (ii) 2 PR₂Cl, THF, -78 °C.

Scheme 9. Reaction of Pd₂(dba)₃ (6**) with Bis(phosphino-*o*-carboranyl)disilane **2**^a**



^a Conditions: (i) Pd₂(dba)₃ (**6**), toluene, 25 °C.

microanalysis data. Indeed, the NMR spectra of the palladium complexes are in complete agreement with an authentic sample of **8** (vide infra).

Although we did not investigate the mechanism in detail, we believe that the phosphine tethers force the Si-Si linkage into the proximity of the metal center by precoordination and this accelerates the oxidative addition. The Si-Si bond then oxidatively adds to the

palladium center by replacement of the dba ligands. The reaction is not restricted to the PR₂ (R = Me (**2a**), OEt (**2b**)) derivatives; the bulkier bis((diphenylphosphino)-*o*-carboranyl)disilane (**2c**) also results in the corresponding *cis*-bis(chelate) **8c** after oxidative addition of the Si-Si bond, but only after extended reaction times.

Conclusions

The use of an *o*-carboranyl unit as the auxiliary ligand backbone was found to result in an increase in the difference in kinetic stability between the *cis* and *trans* isomers, which enabled the isolation and full characterization of **4a,b** and **7a**, all having *trans* structures. Thus, the steric bulkiness of the backbone connecting Si to P in these Cab^{P,Si} systems engenders steric constraints on the metal center that increase the kinetic stability of the metal chelates. Therefore, our examination of the chelate-assisted oxidative addition reactions of the phosphinosilanes has enabled us to reach the following conclusions. Our success in demonstrating the formation of kinetically stabilized *trans*-bis(chelates) relies on the following two factors: (1) the bulkiness of the alkyl groups in the phosphinosilanes and (2) the rapid bis-chelation of the phosphinosilanes with a rigid *o*-carborane backbone. We intend to use these principles as we continue our research into the stereoselectivity of the chelate-assisted oxidative addition reactions of the d¹⁰ metal complexes.

Experimental Section

General Procedures. All manipulations were performed under a dry, oxygen-free nitrogen or argon atmosphere using standard Schlenk techniques or in a Vacuum Atmospheres HE-493 drybox. Diethyl ether, toluene, hexane, and pentane were distilled under nitrogen from sodium/benzophenone. Dichloromethane was dried with CaH₂. Benzene-*d*₆ was distilled under nitrogen from sodium and stored in a Schlenk storage flask until needed. CDCl₃ was predried under CaH₂ and vacuum-transferred. *n*-BuLi (1.6 M in hexanes) and Pd₂(dba)₃ (**6**) were used as received from Aldrich. (PPh₃)₂Pt-(CH₂CH₂) (**3**)²² and Pt(cod)₂ (**9**)²³ were obtained by literature methods. All ¹H (300.1 MHz, measured in CDCl₃), ¹³C (75.4 MHz, measured in CDCl₃), ³¹P (121.4 MHz, measured in CDCl₃), and ²⁹Si NMR spectra (59.60 MHz, measured in CDCl₃) were recorded on a Varian Mercury-300BB spectrometer unless otherwise stated. ¹H and ¹³C NMR chemical shifts are reported relative to Me₄Si and were determined by reference to the residual ¹H or ¹³C solvent peaks. The IR spectra were recorded on a Biorad FTS-165 spectrophotometer. Elemental analyses were performed with a Carlo Erba Instruments CHNS-O EA1108 analyzer.

Preparation of (Phosphino-*o*-carboranyl)silanes **2.** A representative procedure is as follows: to a solution of 0.721 g (5.0 mmol) of *o*-carborane in 20 mL of THF, precooled to -78 °C, was added 3.2 mL of *n*-butyllithium (1.6 M in hexanes). The reaction mixture was warmed to room temperature and stirred for 2 h, whereupon it was transferred, via cannula, to a suspension of 5.5 mmol (1.1 equiv) of chlorodimethylphosphine in 20 mL of Et₂O that was cooled to -78 °C. The resultant yellow mixture was warmed to room temperature and stirred for 2 h. The volatiles were then removed under reduced pressure; the crude mixture was taken up in a minimal amount of Et₂O and the solution filtered through a 1

(22) Hartley, F. R. *Organomet. Chem. Rev., Sect. A* **1970**, *6*, 119.

(23) Spencer, J. L.; Ittel, S. D.; Cushing, M. A., Jr. *Inorg. Synth.* **1979**, *19*, 213.

× 5 cm pad of silica gel on a glass frit. Removal of the volatiles provided the final crude product, which was further crystallized from toluene at $-5\text{ }^{\circ}\text{C}$ to provide pure *o*-carboranyl phosphine **1a** as a colorless solid.

THF (40 mL) and 4.0 mmol of **1a** were added to the reaction flask. The solution was cooled to $-78\text{ }^{\circ}\text{C}$, *n*-butyllithium (2.6 mL, 4.16 mmol, 1.6 M in hexanes) was added. The solution was warmed to room temperature, whereupon a thick suspension of white precipitate formed. After the reaction mixture had been stirred for 1 h at room temperature, it was again cooled to $-78\text{ }^{\circ}\text{C}$ and chlorodimethylsilane (1.1 equiv) was added as a neat liquid. The solution was warmed to $-5\text{ }^{\circ}\text{C}$ very slowly (for over 1 h) and stirred at $-5\text{ }^{\circ}\text{C}$ for a total of 3 h. The volatiles were then removed under reduced pressure; the crude mixture was taken up in a minimal amount of Et₂O and filtered through a 1 × 5 cm pad of silica gel on a glass frit. Removal of the volatiles provided the final crude product, which was further crystallized from toluene at $-5\text{ }^{\circ}\text{C}$ to provide pure ((dimethylphosphino)-*o*-carboranyl)silane (**2a**) as a colorless waxy solid. Yield: 92% (0.966 g, 3.7 mmol). Anal. Calcd for B₁₀C₆H₂₃PSi: C, 27.25; H, 8.77. Found: C, 27.17; H, 8.74. IR (KBr pellet, cm⁻¹): 2966 w, 2909 w (ν_{CH}), 2611 s, 2570 w (ν_{BH}), 2162 w (ν_{SiH}).

2b. A procedure analogous to the preparation of **2a** was used, but starting from chlorodiethoxyphosphine (0.861 g, 5.5 mmol) in benzene. Thus, **2b** was crystallized from toluene at $-5\text{ }^{\circ}\text{C}$. Yield: 89% (1.148 g, 3.6 mmol). Anal. Calcd for B₁₀C₈H₂₇O₂PSi: C, 29.61; H, 8.39. Found: C, 29.51; H, 8.36. IR (KBr pellet, cm⁻¹): 2979 w, 2930 w (ν_{CH}), 2576 s (ν_{BH}), 2165 w (ν_{SiH}).

2c. A procedure analogous to the preparation of **2a** was used, but starting from chlorodiphenylphosphine (1.214 g, 5.5 mmol) in benzene. Thus, **2c** was crystallized from toluene at $-5\text{ }^{\circ}\text{C}$. Yield: 82% (1.209 g, 3.3 mmol). Anal. Calcd for B₁₀C₁₆H₂₇PSi: C, 49.45; H, 7.01. Found: C, 49.26; H, 7.03. IR (KBr pellet, cm⁻¹): 3058 m (ν_{CH}), 2570 s (ν_{BH}), 2170 m (ν_{SiH}).

Synthesis of [η²-(phosphino-*o*-carboranyl)silyl]metal Complexes (Cab^{*P,Si*})₂M. A representative procedure is as follows: toluene (15 mL) was added to a mixture of (PPh₃)₂-Pt(C₂H₄) (**3**; 0.224 g, 0.30 mmol) and **2a** (0.157 g, 0.60 mmol). The mixture was stirred for 3 h, and then the volatile compound was removed under reduced pressure. Extraction of the residue with toluene (20 mL), followed by concentration of the extract to approximately half its volume and cooling to $-5\text{ }^{\circ}\text{C}$, resulted in crystallization of pure *trans*-**4a**. Yield: 73% (0.157 g, 0.22 mmol). Anal. Calcd for B₂₀C₁₂H₄₄P₂PtSi₂: C, 20.08; H, 6.18. Found: C, 20.12; H, 6.22. Mp: 235–237 °C dec. IR (KBr pellet, cm⁻¹): 2960 m, 2903 w (ν_{CH}), 2627 s, 2598 s, 2571 s (ν_{BH}).

trans-4b. A procedure analogous to the preparation of **4a** was used, but starting from **2b** (0.193 g, 0.60 mmol) in toluene. Thus, **4b** was crystallized from toluene at $-5\text{ }^{\circ}\text{C}$. Yield: 76% (0.184 g, 0.23 mmol). Anal. Calcd for B₂₀C₁₆H₅₂O₂P₂Si₂Pt: C, 23.84; H, 6.5. Found: C, 23.90; H, 6.72. Mp: 200–203 °C dec. IR (KBr pellet, cm⁻¹): 2985 w, 2896 w (ν_{CH}), 2611 s, 2566 s (ν_{BH}).

cis-5a. DMAD (0.12 mL, 1.0 mmol) was added to a solution of *trans*-**4a** (0.144 g, 0.20 mmol) in toluene (20 mL), and the mixture was heated for 1 h at 110 °C; conversion into *cis*-**5a**, as monitored by ¹H NMR spectroscopy, was quantitative. The solvent was removed in vacuo and the resulting solid crystallized from toluene at $-5\text{ }^{\circ}\text{C}$ to give 0.138 g (0.19 mmol) of yellow microcrystals (96% yield). Anal. Calcd for B₂₀C₁₂H₄₄P₂-PtSi₂: C, 20.08; H, 6.18. Found: C, 20.15; H, 6.25. Mp: 239–241 °C dec. IR (KBr pellet, cm⁻¹): 2956 w, 2924 w, 2852 w (ν_{CH}), 2607 s, 2568 s (ν_{BH}).

cis-5b. A procedure analogous to the preparation of *cis*-**5a** was used, but starting from *trans*-**4b** (0.161 g, 0.20 mmol) in toluene. Thus, *cis*-**5b** was crystallized from toluene at $-5\text{ }^{\circ}\text{C}$. Yield: 92% (0.148 g, 0.184 mmol). Anal. Calcd for B₂₀C₁₆H₅₂O₂P₂-

Si₂Pt: C, 23.84; H, 6.5. Found: C, 23.91; H, 6.69. Mp: 208–210 °C dec. IR (KBr pellet, cm⁻¹): 2955 w, 2928 w (ν_{CH}), 2577 s (ν_{BH}).

General Procedure for cis-5c and 8. Toluene (20 mL) was added to a mixture of suitable metal reagent (0.30 mmol) and **2** (0.60 mmol, 2 equiv). The mixture was stirred for 12 h, and then the volatile compounds were removed under reduced pressure. Extraction of the residue with toluene (2 × 15 mL), followed by concentration and chromatography on silica with 1:1 hexane/benzene as eluent gave bis(chelates) as yellow solids.

cis-5c. Anal. Calcd for B₂₀C₃₂H₅₂P₂Si₂Pt: C, 39.78; H, 5.42. Found: C, 39.85; H, 5.52. Mp: 245–248 °C dec. IR (KBr pellet, cm⁻¹): 3060 w, 2957 w, 2900 w (ν_{CH}), 2575 s (ν_{BH}).

cis-8a. Anal. Calcd for B₂₀C₁₂H₄₄P₂Si₂Pd: C, 22.91; H, 7.05. Found: C, 22.97; H, 7.10. Mp: 225–228 °C dec. IR (KBr pellet, cm⁻¹): 2959 w, 2917 w (ν_{CH}), 2606 s, 2561 s (ν_{BH}).

cis-8b. Anal. Calcd for B₂₀C₁₆H₅₂O₂P₂Si₂Pd: C, 26.79; H, 7.31. Found: C, 26.85; H, 7.42. Mp: 206–208 °C dec. IR (KBr pellet, cm⁻¹): 2992 w (ν_{CH}), 2603 s, 2567 s (ν_{BH}).

cis-8c. Anal. Calcd for B₂₀C₃₂H₅₂P₂Si₂Pd: C, 43.80; H, 5.97. Found: C, 43.85; H, 6.02. Mp: 225–227 °C dec. IR (KBr pellet, cm⁻¹): 3063 w, 2961 w (ν_{CH}), 2604 s, 2563 s (ν_{BH}).

10a. A solution containing **3** (0.30 mmol) and **2c** (1 equiv) in toluene was stirred for 2 h; conversion into **10a**, as monitored by ¹H NMR spectroscopy, was quantitative. Removal of the volatile material under reduced pressure gave a light yellow oil, to which toluene (5 mL) was added. Cooling the mixture to $-5\text{ }^{\circ}\text{C}$ resulted in precipitation of **10a** as colorless microcrystals. Yield: 89% (0.225 g, 0.27 mmol). Anal. Calcd for B₁₀C₃₄H₄₂P₂SiPt: C, 48.39; H, 5.02. Found: C, 48.44; H, 5.10. Mp: 198 °C dec. IR (KBr pellet, cm⁻¹): 3051 w, 2957 w (ν_{CH}), 2581 s (ν_{BH}), 2029 s (ν_{PH}).

10b. To a 20 mL solution containing **9** (0.3 mmol) in toluene were added sequentially 1 equiv of **1c** and 1 equiv of **2c**, to generate **10b** in quantitative yield. The solution was filtered, the volatiles were removed, and the resulting solid was crystallized from toluene to give colorless microcrystals. Yield: 82% (0.224 g, 0.25 mmol). Anal. Calcd for B₂₀C₃₀H₄₈O₂P₂-SiPt: C, 39.6; H, 5.32. Found: C, 40.01; H, 5.48. Mp: 225 °C dec. IR (KBr pellet, cm⁻¹): 3055 w, 3033 w, 2962 w (ν_{CH}), 2603 s, 2579 s, 2544 s (ν_{BH}), 2034 w, 1992 m (ν_{PH}).

Preparation of the Linear Bis(phosphino)disilane 1,2-Bis(1-PR₂-*o*-carboranyl)-1,1,2,2-tetramethyl-1,2-disilane (R = Me (12a**), OEt (**12b**), Ph (**12c**)).** A representative procedure is as follows: to a solution of 0.806 g (2.0 mmol) of bis(*o*-carboranyl)disilane **11** in 20 mL of THF, precooled to $-78\text{ }^{\circ}\text{C}$, was added 2.5 mL of *n*-butyllithium (1.6 M in hexanes). The reaction mixture was warmed to room temperature and stirred for 2 h, whereupon it was transferred, via cannula, to a suspension of 4.4 mmol (2.2 equiv) of chlorodimethylphosphine in 20 mL of Et₂O that was cooled to $-78\text{ }^{\circ}\text{C}$. The resultant yellow mixture was warmed to room temperature and stirred for 2 h. The volatiles were then removed under reduced pressure; the crude mixture was taken up in a minimal amount of Et₂O and filtered through a 1 × 5 cm pad of silica gel on a glass frit. Removal of the volatiles provided the final crude product, which was further crystallized from toluene at $-5\text{ }^{\circ}\text{C}$ to provide pure bis((dimethylphosphino)-*o*-carboranyl)disilane (**12a**) as a colorless solid. Yield: 70% (0.734 g, 1.4 mmol). Anal. Calcd for B₂₀C₁₂H₄₄PSi₂: C, 27.35; H, 8.42. Found: C, 27.27; H, 8.39. Mp: 225–227 °C. ²⁹Si NMR: δ –9.03. IR (KBr pellet, cm⁻¹): 2982 m, 2910 m (ν_{CH}), 2611 s, 2586 s, 2569 s (ν_{BH}).

12b. A procedure analogous to the preparation of **12a** was used, but starting from chlorodiethoxyphosphine (0.689 g, 4.4 mmol) in benzene. Thus, **12b** was crystallized from toluene at $-5\text{ }^{\circ}\text{C}$. Yield: 62% (0.743 g, 1.2 mmol). Anal. Calcd for B₂₀C₁₆H₅₂O₂PSi₂: C, 31.25; H, 8.53. Found: C, 31.35; H, 8.50. Mp: 230–233 °C. ²⁹Si NMR: δ –8.95. IR (KBr pellet, cm⁻¹): 2975 m, 2940 m (ν_{CH}), 2601 s, 2577 s, 2568 s (ν_{BH}).

12c. A procedure analogous to the preparation of **12a** was used, but starting from chlorodiphenylphosphine (0.971 g, 4.4 mmol) in benzene. Thus, **12c** was crystallized from toluene at $-5\text{ }^{\circ}\text{C}$. Yield: 68% (1.046 g, 1.4 mmol). Anal. Calcd for $\text{B}_{20}\text{C}_{32}\text{H}_{52}\text{PSi}$: C, 49.58; H, 6.77. Found: C, 49.41; H, 6.75. Mp: 247–248 $^{\circ}\text{C}$. ^{29}Si NMR: $\delta -7.19$. IR (KBr pellet, cm^{-1}): 3051 w, 2955 w (ν_{CH}), 2611 w, 2575 s (ν_{BH}).

Reaction of 12 with the Palladium Complex $\text{Pd}_2(\text{dba})_3$ (6). Representative procedure: Toluene (15 mL) was added to a mixture of $\text{Pd}_2(\text{dba})_3$ (**6**; 0.092 g, 0.1 mmol) and **12a** (0.115 g, 0.22 mmol). The mixture was stirred for 3 h, and then the volatile compounds were removed under reduced pressure. Extraction of the residue with toluene (20 mL), followed by concentration of the extract to approximately half its volume and cooling to $-5\text{ }^{\circ}\text{C}$, resulted in crystallization of pure *cis*-**8a**. Yield: 84% (0.107 g, 0.17 mmol).

cis-8b. A procedure analogous to the preparation of *cis*-**8a** was used, but starting from **12b** (0.122 g, 0.22 mmol) in toluene. Thus, *cis*-**8b** was crystallized from toluene at $-5\text{ }^{\circ}\text{C}$. Yield: 81% (0.115 g, 0.16 mmol).

cis-8c. A procedure analogous to the preparation of *cis*-**8a** was used, but starting from **12c** (0.170 g, 0.22 mmol) in toluene. Thus, *cis*-**8c** was crystallized from toluene at $-5\text{ }^{\circ}\text{C}$. Yield: 86% (0.150 g, 0.17 mmol).

Crystal Structure Determination. Crystals of **4a**, **5a,c**, **8c**, and **10a,b** were obtained from toluene, sealed in glass capillaries under argon, and mounted on the diffractometer. Data were collected and corrected for Lorentz and polarization effects. Each structure was solved by the application of direct methods using the SHELXS-96 program^{24a} and least-squares refinement using SHELXL-97.^{24b} After anisotropic refinement of all non-H atoms, several H atom positions could be located in difference Fourier maps. These were refined isotropically, while the remaining H atoms were calculated in idealized positions and included in the refinement with fixed atomic contributions. Further detailed information is given in Table 3.

Computational Details. Stationary points on the potential energy surface were calculated using the Amsterdam Density Functional (ADF) program, developed by Baerends et al.^{25,26} and vectorized by Ravenek.²⁷ The numerical integration scheme applied for the calculations was developed by te Velde et al.^{28,29} The geometry optimization procedure was based on the method due to Versluis and Ziegler.³⁰ The electronic

configurations of the molecular systems were described by double- ζ STO basis sets with polarization functions for the H, B, and C atoms, while triple- ζ Slater type basis sets were employed for the Si, P, and Pt atoms.^{31,32} The 1s electrons of B and C, the 1s–2p electrons of Si and P, and the 1s–4d electrons of Pt were treated as frozen cores. A set of auxiliary³³ s, p, d, f, and g STO functions, centered on all nuclei, was used in order to fit the molecular density and the Coulomb and exchange potentials in each SCF cycle. Energy differences were calculated by augmenting the local exchange–correlation potential by Vosko et al.³⁴ with Becke's³⁵ nonlocal exchange corrections and Perdew's³⁶ nonlocal correlation corrections (BP86). Geometries were optimized including nonlocal corrections at this level of theory. First-order Pauli scalar relativistic corrections^{37,38} were added variationally to the total energy for all systems. In view of the fact that all systems investigated in this work show a large HOMO–LUMO gap, a spin-restricted formalism was used for all calculations. No symmetry constraints were used.

Acknowledgment. We are grateful to the Korea Research Foundation (Grant No. KRF-2002-015-CP0200) for their financial support.

Supporting Information Available: Crystallographic data (excluding structure factors) for the structures **4a**, **5a,c**, **8c**, and **10a,b** reported in this paper and listings giving optimized geometries of the crucial structures (**4a** and **5a**) reported (Cartesian coordinates, in Å); crystallographic data are also available in electronic form as CIF files. This material is available free of charge via the Internet at <http://pubs.acs.org>.

OM034112L

(28) te Velde, G.; Baerends, E. J. *J. Comput. Chem.* **1992**, *99*, 84.

(29) Boerrigter, P. M.; te Velde, G.; Baerends, E. J. *Int. J. Quantum Chem.* **1988**, *33*, 87.

(30) Versluis, L.; Ziegler, T. *J. Chem. Phys.* **1988**, *88*, 322.

(31) Snijders, J. G.; Baerends, E. J.; Vernoijs, P. *At. Nucl. Data Tables* **1982**, *26*, 483.

(32) Vernoijs, P.; Snijders, J. G.; Baerends, E. J. *Slater Type Basis Functions for the Whole Periodic System*; Internal Report (in Dutch); Department of Theoretical Chemistry, Free University: Amsterdam, The Netherlands, 1981.

(33) Krijn, J.; Baerends, E. J. *Fit Functions in the HFS Method*; Internal Report (in Dutch); Department of Theoretical Chemistry, Free University: Amsterdam, The Netherlands, 1984.

(34) Vosko, S. H.; Wilk, L.; Nusair, M. *Can. J. Phys.* **1980**, *58*, 1200.

(35) Becke, A. *Phys. Rev. A* **1988**, *38*, 3098.

(36) (a) Perdew, J. P. *Phys. Rev. B* **1986**, *34*, 7406. (b) Perdew, J. P. *Phys. Rev. B* **1986**, *33*, 8822.

(37) Snijders, J. G.; Baerends, E. J. *Mol. Phys.* **1978**, *36*, 1789.

(38) Snijders, J. G.; Baerends, E. J.; Ros, P. *Mol. Phys.* **1979**, *38*, 1909.

(24) (a) Sheldrick, G. M. *Acta Crystallogr., Sect. A* **1990**, *A46*, 467. (b) Sheldrick, G. M. SHELXL, Program for Crystal Structure Refinement; University of Göttingen, Göttingen, Germany, 1997.

(25) Baerends, E. J.; Ellis, D. E.; Ros, P. *Chem. Phys.* **1973**, *2*, 41.

(26) Baerends, E. J.; Ros, P. *Chem. Phys.* **1973**, *2*, 52.

(27) Ravenek, W. In *Algorithms and Applications on Vector and Parallel Computers*; te Riele, H. J. J., Dekker, T. J., van de Horst, H. A., Eds.; Elsevier: Amsterdam, The Netherlands, 1987.